Photochemistry and Photobiology, 2003, 78(3): 290–297

Initial Characterization of the Primary Photochemistry of AppA, a Blue-light–using Flavin Adenine Dinucleotide–domain Containing Transcriptional Antirepressor Protein from *Rhodobacter sphaeroides*: A Key Role for Reversible Intramolecular Proton Transfer from the Flavin Adenine Dinucleotide Chromophore to a Conserved Tyrosine?¶

Wouter Laan[1], Michael A. van der Horst[1], Ivo H. van Stokkum[2] and Klaas J. Hellingwerf*[1]

[1]Laboratory for Microbiology, Swammerdam Institute for Life Sciences, BioCentrum Amsterdam, University of Amsterdam, The Netherlands
[2]Division of Physics and Astronomy, Faculty of Sciences, Vrije Universiteit, Amsterdam, The Netherlands

Received 27 March 2003; accepted 11 June 2003

ABSTRACT

The flavin adenine dinucleotide (FAD)–containing photoreceptor protein AppA (in which the FAD is bound to a novel so-called BLUF domain) from the purple nonsulfur bacterium *Rhodobacter sphaeroides* was previously shown to be photoactive by the formation of a slightly redshifted long-lived intermediate that is thought to be the signaling state. In this study, we provide further characterization of the primary photochemistry of this photoreceptor protein using UV–Vis and Fourier-transform infrared spectroscopy, pH measurements and site-directed mutagenesis. Available evidence indicates that the FAD chromophore of AppA may be protonated in the receptor state, and that it becomes exposed to solvent in the signaling state. Furthermore, experimental data lead to the suggestion that intramolecular proton transfer (that may involve [anionic] Tyr-17) forms the basis for the stabilization of the signaling state.

INTRODUCTION

Regulation of expression of the photosynthetic machinery of purple nonsulfur anoxyphotobacteria such as *Rhodobacter sphaeroides* is a complex process, with multiple signal transduction pathways and transcriptional regulators being involved (1–3). One such regulator is the flavin adenine dinucleotide (FAD)–binding transcriptional antirepressor protein AppA, which interacts with the PpsR repressor protein to contribute to regulation of the expression of the *puc, puf, bch* and *crt* operons. These regulatory proteins are multifunctional in the sense that they coordinate the input of both light- and redox-derived signals, the latter originating primarily via variations in the amount of available oxygen.

The N-terminal domain of AppA, which binds FAD, appears dispensable in the redox-sensitive interaction of this antirepressor with PpsR (4). Surprisingly, the redox transitions in AppA are not based on the flavin moiety but rather on a cysteine-rich motif in its C-terminal domain. In contrast, the FAD moiety appears to be involved in the persistent phase of blue-light–mediated repression of the transcription of photosynthetic genes, as first observed by Shimada *et al*. (5). Consistent with this is the report of Masuda and Bauer (6) that AppA can be activated with light to form a long-lived signaling state with a slightly (~10 nm) redshifted absorption spectrum. In this signaling state, AppA undergoes significant conformational change, which strongly modulates its interaction with PpsR, thus providing an explanation for the blue-light–mediated repression of the genes of *R. sphaeroides*, which encode its photosynthesis machinery.

Recent detailed sequence analyses, and the use of programs to predict secondary structure (7), have revealed that the FAD-binding domain of AppA may actually represent a new type of flavin-binding fold that is structurally distinct from all known flavin-binding folds, both within and beyond known photoreceptor families. This domain has tentatively been named the BLUF (blue-light–using FAD) domain. Preliminary characterization of the photochemistry of AppA supports the unique characteristics of this domain. With respect to both its predicted secondary structure and the known characteristics of its photochemistry, it is very different from the light, oxygen or voltage (LOV) domain of the phototropins, its nearest relative among the photoreceptor families (8,9).

Sequences encoding putative BLUF domains have been identified in proteobacteria, cyanobacteria and the green alga *Euglena gracilis* (7). Many of these BLUF domains are part of multidomain proteins involved in catalytic conversion of the regulatory cyclic nucleotides cyclic adenosine 3′5′monophosphate and bis-(3′,5′)-cyclic diguanylate, a regulatory ''alarmone'' (7) of particular relevance to the bacterial domain. Within such multidomain proteins the BLUF domains presumably function as regulatory domains, modulating the catalytic activity of these nucleotide-converting enzymes in response to the absorption of

---

¶Posted on the website on 1 July 2003

*To whom correspondence should be addressed at: Laboratory for Microbiology, Swammerdam Institute for Life Sciences, Nieuwe Achtergracht 166, Amsterdam 1018 WV, The Netherlands; e-mail: k.hellingwerf@science.uva.nl

Abbreviations: BLUF, blue-light–using flavin adenine dinucleotide; FAD, flavin adenine dinucleotide; FMN, flavin mononucleotide; FTIR, Fourier-transform infrared; LOV domain, light, oxygen or voltage domain; PAC, photoactivated adenylyl cyclases; PCR, polymerase chain reaction; PYP, photoactive yellow protein; SAS, species (or states)-associated spectra.

blue photons. As with the individual domains of many other multidomain proteins, however, BLUF domains can also be present as small self-contained single-domain proteins. ORF729-1178 from *Klebsiella pneumoniae* exemplifies that possibility. In agreement with the above, the BLUF domain–containing proteins from *E. gracilis* have been demonstrated to be blue-light–activated adenylyl cyclases (photoactivated adenylyl cyclases [PAC] [10]).

In view of the unique structural and functional features of AppA, characterization of its photochemical activation, and of the subsequent formation of its signaling state, is of particular interest. As previously mentioned, a brief pulse of blue light generates a long-lived ($t_{1/2}$ = hundreds of seconds) intermediate that is thought to be the signaling state of AppA. The most striking difference between this state and the receptor state (which is stable in the dark) is a small (~10 nm) redshift of the absorption spectrum of the FAD chromophore. Furthermore, molecular sieve chromatography has revealed a measurable difference in the radius of gyration of the receptor and signaling states of AppA, with the signaling state having the largest radius of gyration (6). The BLUF domains bind FAD noncovalently, as the LOV domains bind flavin mononucleotide (FMN), in an occluded pocket that is shielded from the solvent. Surprisingly, the fluorescence excitation spectrum of the PAC proteins does not show vibrational fine structure (10). This contrasts, however, with the fluorescence properties of all LOV domains and the absorption characteristics of the AppA protein from *R. sphaeroides* (6).

The UV–Vis absorbance characteristics of the putative signaling state of the BLUF domain differ from those of the signaling states of all other known photoreceptor proteins. This suggests that the BLUF domain displays an entirely new type of primary photochemistry, different not only from the well-known *E/Z* photoisomerization of rhodopsins, phytochromes and xanthopsins but also from the FMN–cysteinyl adduct formation characteristic of the LOV domains of phototropins.

In this study, we present data that may indicate that the FAD chromophore of AppA is protonated in the receptor state and deprotonated in the signaling state (as deduced from Fourier-transform infrared [FTIR] spectra), and that the conserved tyrosine in the N-terminus of AppA is crucial for wild-type photochemistry. The FAD chromophore appears to be occluded both in the receptor and in the signaling states of AppA, albeit to a smaller extent in the latter state.

MATERIALS AND METHODS

Strains and growth conditions. Cloning and heterologous overexpression of the N-terminal domain of AppA were performed in *Escherichia coli*, grown in Luria–Bertani or P-broth medium (containing 20 g L^{-1} tryptone, 10 g L^{-1} yeast extract, 5 g L^{-1} dextrose, 5 g L^{-1} NaCl and 8.7 g L^{-1} K_2HPO_4, pH 7.0), using established protocols. Ampicillin and kanamycin were used at 100 and 50 μg mL^{-1}, respectively.

Plasmid construction. Using genomic DNA from *R. sphaeroides* 2.4.1. strain RK1 as a template, the DNA fragment coding for amino acids 5–125 of AppA was amplified with the sense primer AppA5125F, 5′-GCACGGATCC*GATGACGATGACAAA*CTCGAGGCGGACGTCACG-3′ (*Bam*HI restriction site underlined, enterokinase site in italics) and the antisense primer AppA5125R, 5′-GCTTAAGCTTACTGCCGGCTCTCGGCCAG-3′ (*Hin*dIII site underlined). The *Bam*HI–*Hin*dIII-digested polymerase chain reaction (PCR) product was ligated to *Bam*HI–*Hin*dIII-digested pQE30 to yield the plasmid $pQEAppA_{5–125}$. The construct was verified by sequencing (BaseClear, Leiden, The Netherlands).

Site-directed mutagenesis. The Y17I mutant was constructed with the QuickChange site-directed mutagenesis kit (Stratagene, La Jolla, CA). $pQEAppA_{5–125}$ was used as the template for PCR, and the primer sequences were 5′-CTGGTTTCCTGCTGCATTCGCAGCCTGGCGGC-3′ and 5′-GCCGCCAGGCTGCGAATGCAGCAGGAAACCAG-3′. The construct was verified by sequencing (BaseClear).

Protein expression and purification. E. coli M15 pREP4, transformed with $pQEAppA_{5–125}$, was grown in P-broth medium containing kanamycin (50 μg mL^{-1}) and ampicillin (100 μg mL^{-1}) at 30°C. When the culture reached an optical density of 0.6 at a wavelength of 600 nm, protein expression was induced by adding 0.4 m*M* isopropyl-thio-β-D-galactoside. Growth was allowed to continue for 16 h before the cells were harvested by centrifugation, resuspended in ice-cold lysis buffer (50 m*M* Tris–HCl, pH 8.0, 150 m*M* NaCl, 0.1% [wt/vol] Triton-X100, 15% glycerol and 1 m*M* PefaBloc) and treated with deoxyribonuclease (30 μg mL^{-1}), ribonuclease (30 μg mL^{-1}) and lysozyme (1 mg mL^{-1}). Held on ice for 30 min, the suspension was subsequently sonicated (with a 50% duty cycle) and centrifuged at 16 000 rpm for 45 min. The soluble fraction was applied to a Ni–nitrilotriacetic acid–agarose column, the column was washed with 50 m*M* Tris–HCl, pH 8.0, 500 m*M* NaCl and 20 m*M* imidazol, and AppA was eluted with 50 m*M* Tris–HCl, pH 8.0, 500 m*M* NaCl and 250 m*M* imidazol. The eluted protein was dialysed against 50 m*M* Tris–HCl, pH 7.8, 500 m*M* NaCl and 1 m*M* ethylenediaminetetraacetic acid and stored in the dark at 4°C. Protein concentrations were determined based on the assumption that the extinction coefficient of 11.3 mM^{-1} cm^{-1} at 450 nm of free FAD (11) is equal to that of protein-bound FAD. Purity of the samples was checked with sodium dodecyl sulfate–polyacrylamide gel electrophoresis.

Fourier-transform infrared spectroscopy. AppA was concentrated to about 600 μ*M* in 10 m*M* Tris–HCl, pH 8.0, using a Microcon filter. A 10 μL sample was placed on a CaF_2 window and dried under vacuum. This was repeated several times, after which the dried protein was resuspended in 20 μL of 10 m*M* Tris–HCl, pH 8.0. The rehydrated sample was then sandwiched between this and a second CaF_2 window, using a 12 μm polyethylene spacer. Measurements were performed on a Bio-Rad FTS 60A spectrometer, equipped with a KBr beam splitter and a liquid nitrogen–cooled mercury–cadmium–telluride detector. The spectra were recorded at 20°C with a resolution of 2 cm^{-1} and are averages of 762 scans. The spectra were corrected for water vapor and instrument drift, without further smoothing. To convert AppA from the receptor to the signaling state, the sample was illuminated for 2 min using a 450 W xenon-arc lamp (XBO-450 OFR, Osram, München, Germany) in a LAX 1450 lamp housing (Müller Elektronik-Optik, Moosinning, Germany) equipped with a long-pass filter 5146 (>345 nm, Oriel, Stanford, UK). After passing a water filter (Oriel liquid filter), the light was guided into a glass fiber optic bundle by an Oriel fiber bundle–focusing assembly. The fiber bundle was led into the sample compartment of the spectrometer, illuminating the sample under an angle of approximately 30°.

FTIR spectra of protonated and deprotonated FAD were obtained using a solution of 20 m*M* FAD in 10 m*M* citrate buffer, pH 5.0, and in 0.1 *M* NaOH, respectively.

Simultaneous transient UV–Vis absorption and pH measurements. Absorption and pH signals were measured simultaneously by placing a ''Kraayenhof vessel'' (12) in the sample compartment of a Hewlett Packard 8453 spectrophotometer (Portland, OR). Two of the four available ports of the vessel were used for the measuring beam of the spectrophotometer, and a third one was used for a Mettler Toledo micro (combination)-electrode (InLab423) connected to a Dulas Engineering amplifier. The amplified signal was fed into a linear strip-chart recorder (Kipp & Zonen, Delft, The Netherlands, type BD41). Continuous actinic illumination was provided through the fourth port of the vessel from a Schott KL1500 light source (containing a 150 W halogen lamp). To avoid heating of the sample, the light was filtered through a band-pass filter (450 nm, full-width half-maximum 10 nm). pH changes were converted to moles of protons by calibration with microliter amounts of 2.5 m*M* oxalic acid.

AppA was used at a concentration of 110 μ*M* in a working volume of 1.9 mL, using an unbuffered solution of 1 *M* KCl. pH titrations of FAD (in 1 *M* KCl) and AppA (in 10 m*M* Tris) were carried out by adding microliter amounts of 1 *M* NaOH or HCl solution. The titration data were analyzed using the Henderson–Hasselbalch equation.

For measurement of the rate of receptor state recovery, AppA (~20 μ*M* in 10 m*M* Tris–HCl, pH 8, 9, 10 or 11) was irradiated with saturating actinic white light from the Schott KL1500 light source and allowed to revert to the receptor state in the dark. Spectra were recorded every 120 s for 45 min. The absorption changes at 410, 420 and 444 nm were analyzed by mono and biexponential fits to the data using Origin software (Microcal Software Inc., Northampton, MA). Global analysis of the time-gated spectra (13) was performed using a sequential model: 1 → 2 → 3. The estimated model

```
           L  E  A  D  V  T  M  T  G  S  D  L  V  S  C  C  Y  R  S  L  A  A  P  D  L  T
N-AppA 5'  CTCGAGGCGGACGTCACGATGACGGGCTCGGATCTGGTTTCCTGCTGCTACCGCAGCCTGGCGGCCCCGGATCTGACG
L42555 5'  CTCGAGGCGGACGTCACGATGACGGGCTCGGATCTGGTTTCCTGCTGCTACCGCAGCCTGGCGGCCCCGGATCTGACG
           L  E  A  D  V  T  M  T  G  S  D  L  V  S  C  C  Y  R  S  L  A  A  P  D  L  T

           L  R  D  L  L  D  I  V  E  T  S  Q  A  H  N  A  R  A  Q  L  T  G  A  L  F  Y
N-AppA     CTGCGCGACCTCCTCGACATCGTCGAGACCTCGCAGGCGCACAATGCCCGGGCGCAGCTGACCGGCGCGCTCTTCTAC
L42555     CTGCGCGACCTCCTCGACATCGTCGAGACCTCGCAGGCGCACAATGCCCGGGCGCAGCTGACCGGCGCGCTCTTCTAC
           L  R  D  L  L  D  I  V  E  T  S  Q  A  H  N  A  R  A  Q  L  T  G  A  L  F  Y

           S  Q  G  V  F  F  Q  W  L  E  G  H  P  A  A  V  A  E  V  M  S  H  I  Q  R  D
N-AppA     AGTCAGGGCGTCTTCTTCCAGTGGCTCGAAGGCCACCCCGCCGCCGTGGCGGAGGTCATGAGCCACATCCAGCGGGAC
L42555     AGCCAGGGCGTCTTCTTCCAGTGGCTCGAAGGCCGCCCCGCCGCCGTGGCGGAGGTCATGACCACATCCAGCGGGAC
           S  Q  G  V  F  F  Q  W  L  E  G  R  P  A  A  V  A  E  V  M  T  H  I  Q  R  D

           R  R  H  S  N  V  E  I  L  A  E  E  S  I  A  K  R  R  F  A  G  W  H  M  Q  L
N-AppA     CGGCGCCACAGCAACGTCGAGATCCTGGCAGAGGAATCGATCGCCAAGCGCCGCTTTGCGGGATGGCACATGCAGCTC
L42555     CGGCGCCACAGCAACGTCGAGATCCTGCGCAGAGGAACCGATCGCCAAGCGCCGCTTTGCGGGATGGCACATGCAGCTC
           R  R  H  S  N  V  E  I  L  A  E  E  P  I  A  K  R  R  F  A  G  W  H  M  Q  L

           S  C  S  E  A  D  M  R  S  L  G  L  A  E  S  R  Q
N-AppA     TCCTGCTCGGAGGCCGACATGCGCAGCCTCGGGCTGGCCGAGAGCCGGCAG 3'
L42555     TCCTGCTCGGAGGCCGACATGCGCAGCCTCGGGCTGGCCGAGAGCCGGCAG 3'
           S  C  S  E  A  D  M  R  S  L  G  L  A  E  S  R  Q
```

Figure 1. Sequence alignment of the N-terminal domain of AppA from two strains of *R. sphaeroides* (*i.e.* 2.4.1. and RK1). The sequence of the cloned PCR fragment was aligned with the deposited sequence (accession no. L42555) using Clustal W (http://www.ebi.ac.uk/clustalw/). Base pair and resulting amino acid substitutions are highlighted in reverse contrast. The conserved tyrosine (#17), target for site-directed mutagenesis in this study, has been circled and is represented in bold.

parameters are the lifetimes and species (or state)-associated spectra (SAS) of states 1, 2 and 3.

RESULTS

The N-terminal domain of AppA from *R. sphaeroides* RK1

To obtain an expression plasmid for the flavin-containing N-terminal domain of AppA, a DNA fragment encoding amino acids 5–125 was amplified by PCR using chromosomal DNA of *R. sphaeroides* RK1 (14) and subsequently cloned in *E. coli* (see Materials and Methods). Surprisingly, the sequence of the DNA fragment obtained contained five single–base pair substitutions as compared with the sequence of the corresponding domain of AppA from *R. sphaeroides* strain HR, deposited in the database (accession number L42555; see also Fig. 1). Repetitive PCR amplification and subsequent sequencing confirmed that the sequence differences are not the result of PCR errors but are specific to the *Rhodobacter* strain used. Only three of the DNA substitutions lead to changes at the protein level: R64H, T72S and P92S (numbering according to the sequence of the amplified fragment of RK1); the other two are silent mutations. The three substituted amino acids do not belong to the conserved residues in BLUF domains (7); they also do not seem to have an identifiable effect on the FAD binding nor the spectral properties of AppA.

The photocycle of AppA: kinetics and SAS

In contrast to the observation of Masuda and Bauer (6), our initial analyses indicated that the signaling state of AppA from *R. sphaeroides* RK1 can also be formed, albeit less efficiently, with light <300 and >500 nm (data not shown). The spectra of the receptor and the signaling states obtained, however, are very similar to those of the HR strain (see Fig. 2a). The absorbance maximum of the long-wavelength absorbance band of the flavin is at 444 and 458 nm for the receptor and signaling state, respectively. This may be compared to 449 and 454 nm of free flavin, which undergoes a deprotonation of the N_3 atom of the isoalloxazine ring in aqueous solution, with a pK_a of 10.1 (15). Titration of AppA through the pH range from 7.5 to 14, with simultaneous measurement of absorbance spectra, reveals that the pK_a of the FAD chromophore in the AppA protein has shifted to a value of 11.7 (displaying the typical more strongly cooperative transition of a protein-bound chromophore, *i.e.* with an n value of 1.4 and 0.6 for free and protein-bound flavin, respectively). These observations suggest that in the physiological pH range, the receptor state of AppA contains a protonated flavin.

Blue light activates signaling state formation in AppA over a wide range of pH values, from 7 to values higher than 11. Under acidic pH conditions, AppA is not soluble in the buffer systems tested. The spectrum of the long-lived putative signaling intermediate of AppA shows, besides a shift to longer wavelengths (see further below), one notable feature: the flavin vibrational fine structure at the high-energy side of the main UV–Vis transition (*i.e.* from 400 to 430 nm) is lost in this state (see *e.g.* Fig. 2). However,

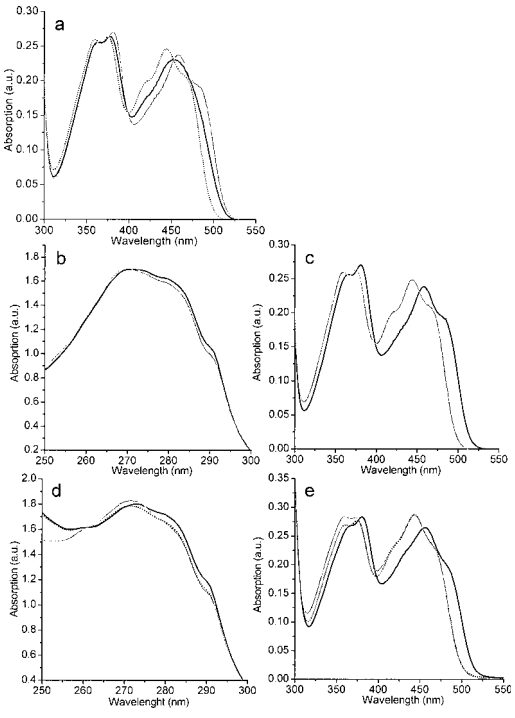

Figure 2. Time dependence of the recovery of the receptor state of AppA (a) and SAS that have a role in this process (b–e). AppA was converted to the signaling state by illumination with white light and allowed to revert to the receptor state in the dark. a: Spectra of the signaling state (gray), 10 min after switching off the actinic illumination (black) and of the receptor state (dotted). The pH in this experiment was 8.0. b,c: SAS at pH 8.0: spectra of the state with a lifetime of 1043 s (black) and the receptor state (gray). d,e: SAS at pH 11.0: spectra of the states with lifetimes of 307 s (black) and 4800 s (dotted) and the receptor state (gray) a.u., absorption units.

Table 1. pH dependence of the rate of dark recovery of AppA. The rate of the dark recovery of the receptor state at different pH was determined by fitting a plot of the absorbance changes at 444 nm with a monoexponential decay function with Origin software

pH	Rate ($\times 10^{-3}$ s^{-1})
8.0	1.02 ± 0.04
9.0	1.07 ± 0.02
10.0	1.28 ± 0.03
11.0	3.34 ± 0.04

because the low-energy fine structure persists, it is difficult to conclude to what extent the flavin is more extensively exposed to polar solvent in this state. The rate of the recovery reaction is slightly pH dependent. This process accelerates approximately three-fold on an increase in pH from 8 to 11 (*i.e.* from $1 \cdot 10^{-3}$ s^{-1} to $3 \cdot 10^{-3}$ s^{-1} when fitted monoexponentially, Table 1). At alkaline pH, recovery of the receptor state is no longer monoexponential. Under these conditions it is most optimally fit with a biexponential function. At pH 11 the recovery rates are $3.4 \cdot 10^{-3}$ s^{-1} and $0.7 \cdot 10^{-3}$ s^{-1} for the fast and slow phase of the reaction, respectively (Table 2).

An initial inspection of the spectra (*e.g.* see the 10 min spectrum in Fig. 2a) may lead one to conclude that the vibrational fine structure is lost completely. Detailed (global) analysis, however, shows that this is not the case. The SAS obtained during the recovery process do show this fine structure (Fig. 2c,e); they show only small differences in the high-energy flavin absorption band (*i.e.* in the range from 320 to 420 nm) and in the UV region (Fig. 2b,d). It is possible that the mixture of the two states present at the intermediate time points blurs visibility of the fine structure. Changes in the protonation state of a tyrosine side chain might contribute to these signals (see Fig. 3 and further below).

Analysis of the signaling state and receptor state UV–Vis difference spectrum

As noted by Masuda and Bauer (6), the difference spectrum between signaling and receptor states of AppA suggests that light induces a redshift in the flavin spectrum. The analysis in Fig. 3a confirms that a difference spectrum of a modeled isoenergetic shift of the spectrum of the receptor state of AppA reproduces the difference spectrum rather well in the visible part of the spectrum, including the fine structure at 460, 430, 360 and 345 nm. Nevertheless, there is a strong deviation between the two spectra in the UV region: whereas the predicted difference spectrum shows large amplitudes in the 250–325 nm region, the observed difference spectrum actually shows much smaller amplitudes (Fig. 3b). This may be caused by additional, compensating, absorbance changes in this spectral region, such as a decrease in the region around 295 nm and an increase at 274 nm. Such changes may be caused by a simultaneous phenolate to phenol transition, for example in tyrosine.

A role for Y17 in the photocycle of AppA

On the basis of experimental evidence that indicates that the receptor state of AppA contains, or may contain, a protonated flavin and data illustrating that spectral changes occur in the UV region during transition to the signaling state, it is possible to speculate that a tyrosinate may be involved in the photocycle of AppA, *e.g.* as a transient acceptor of a proton donated by the flavin. We thus replaced the strictly conserved (that is, in the BLUF family) Y17 of AppA (*i.e.* Y21 in the numbering of Gomelsky and Klug [7]) with an isoleucine and produced and purified the Y17I variant through heterologous expression in *E. coli* (for further details see Materials and Methods). Figure 4 shows that by following this procedure, an authentically colored protein is formed. The visible spectrum of the Y17I variant is in shape rather similar to that of the receptor state from the wild-type derivative but, overall, slightly (*i.e.* 4 nm) blueshifted with an altered (*i.e.* decreased) intensity ratio of the high- over the low-energy absorption band of the flavin and the absence of vibrational fine structure in the region from 400 to 430 nm. Importantly, this derivative turned out to be completely inactive in photocycling under all illumination conditions tested.

FTIR analyses of light-induced difference spectra of AppA

Because of the possibility that changes in the protonation state of the flavin may accompany the photocycle transitions in AppA, we used static light–induced FTIR difference spectroscopy for its further characterization. Because the recovery rate of the receptor state of AppA is slow, it is relatively straightforward to convert the photoreceptor protein into a high steady-state concentration of its signaling state with actinic illumination. To confirm the quantitative conversion of AppA to the signaling state under the conditions of the FTIR measurements, UV–Vis measurements were carried out in parallel (data not shown).

The FTIR difference spectrum obtained (Fig. 5) shows many features in the range from 1000 to 1800 cm^{-1}, which is dominated (*i.e.* by having the largest difference extinction coefficient) by a band shift from 1710 to 1698 cm^{-1}. This latter feature can be assigned to the C=O of the C_4 atom of the isoalloxazine ring (16,17). This is confirmed by the comparison between the light-induced FTIR difference spectrum and the FTIR spectra of free FAD in buffer at acidic and alkaline pH (see spectra I and III in Fig. 5b). These FTIR spectra of FAD in the protonated and deprotonated states may also explain many features in the light-

Table 2. Mono- versus biexponential decay of the receptor state of AppA as a function of pH. Data deconvolution was performed both at single wavelengths and by global analysis. A_1 and A_2 are the amplitudes of the fast and slow components, respectively. The values for the single wavelength analysis are the average from recordings at 410 and 420 nm

	Single wavelength[a]				Global analysis[a]	
pH	$Rate_1$ ($\times 10^{-3}$ s^{-1})	A_1 (%)	$Rate_2$ ($\times 10^{-3}$ s^{-1})	A_2 (%)	$Rate_1$ ($\times 10^{-3}$ s^{-1})	$Rate_2$ ($\times 10^{-3}$ s^{-1})
8.0	1.01 ± 0.01	100	NA	NA	0.96	NA
11.0	3.43 ± 0.06	82 ± 3	0.66 ± 0.2	18 ± 3	3.26	0.21

[a] not applicable.

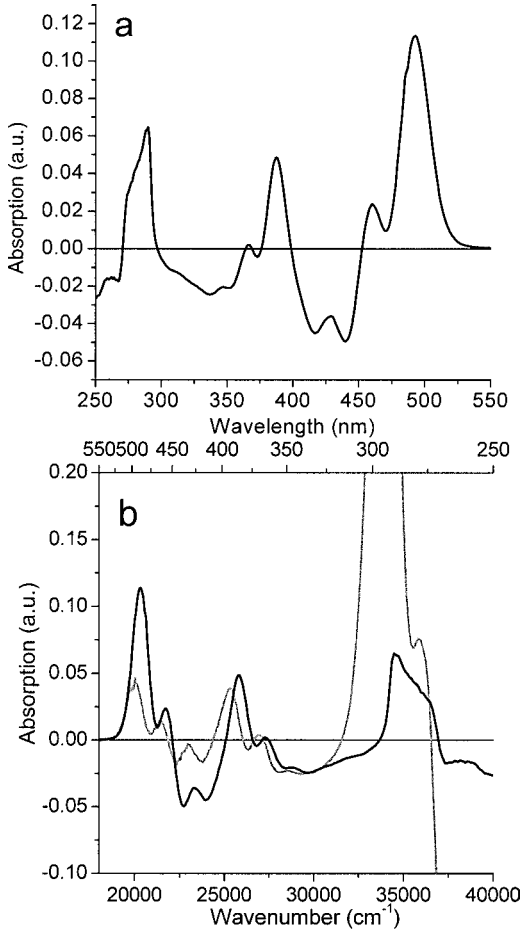

Figure 3. AppA difference spectra (+/– illumination) in the UV–Vis region. a: AppA difference spectrum as a function of wavelength. b: AppA difference spectrum as a function of wavenumber (black) and the difference spectrum of a simulated 800 cm^{-1} redshifted ground-state spectrum minus the ground-state spectrum (gray). a.u., absorption units.

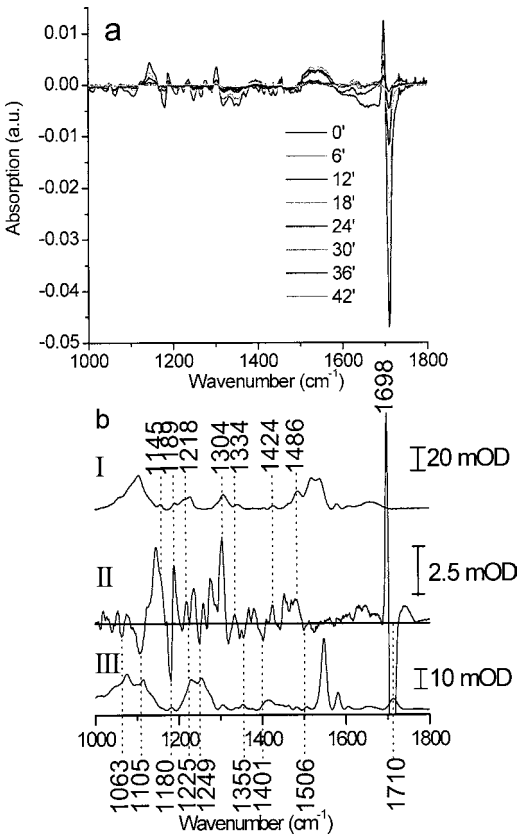

Figure 5. Initial FTIR characterization of AppA. a: FTIR difference spectra measured every 6 min during dark reversion of the signaling state. b: Comparison of the light-induced difference spectrum of AppA (II) with the FTIR spectra of deprotonated (I) and protonated (III) FAD in aqueous buffer (NaOH–citrate) at high (I) and low (III) pH, respectively. The vertical dotted lines correspond to the frequency of the negative and positive bands of the AppA difference spectrum, which align with bands in the spectra of protonated and deprotonated FAD, respectively. a.u., absorption units.

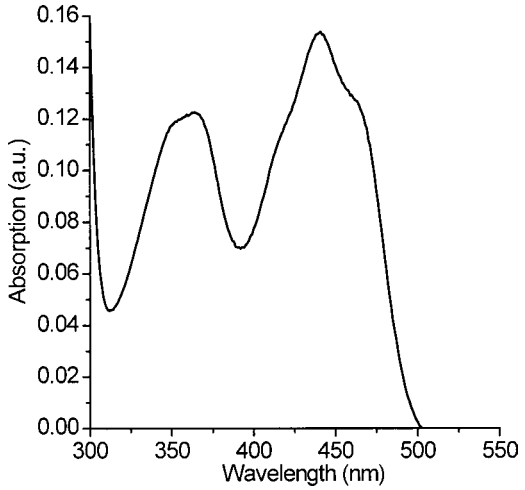

Figure 4. UV–Vis spectrum of the Y17I variant of AppA. This spectrum was recorded in 10 m*M* Tris–HCl at pH 8.0 and room temperature. a.u., absorption units.

induced difference spectrum in the region from 1000 to 1600 cm^{-1}. In this same spectral region, contributions from a change in protonation state of a tyrosinate would be expected. Close inspection of this region shows that at some (but not all) of the expected positions changes do occur (*e.g.* at 1451 and 1443 cm^{-1}).

Test of light-induced proton release by AppA

In many photoreceptor proteins, proton transfer accompanies light activation. This can be either to an intramolecular or external acceptor (*e.g.* the buffer; see for instance Sasaki and Spudich [18]). Besides protons from the chromophore, Bohr protons may be released because of the conformational transitions associated with signal generation (see, *e.g.* responses in photoactive yellow protein [PYP] and Cph1). Because the FTIR difference spectra of AppA indicate that proton transfer is involved in photoactivation of the photoreceptor protein, we tested whether protons are released into the solvent on blue-light illumination of AppA. The results obtained (Fig. 6) reveal that no significant proton release occurs (*i.e.* less than 0.07 H^+/AppA, as can be deduced from a comparison with the size of the calibration pulse) on signaling state formation. The use of blue light in this experiment is important because white light illumination caused significant heating artifacts. The latter

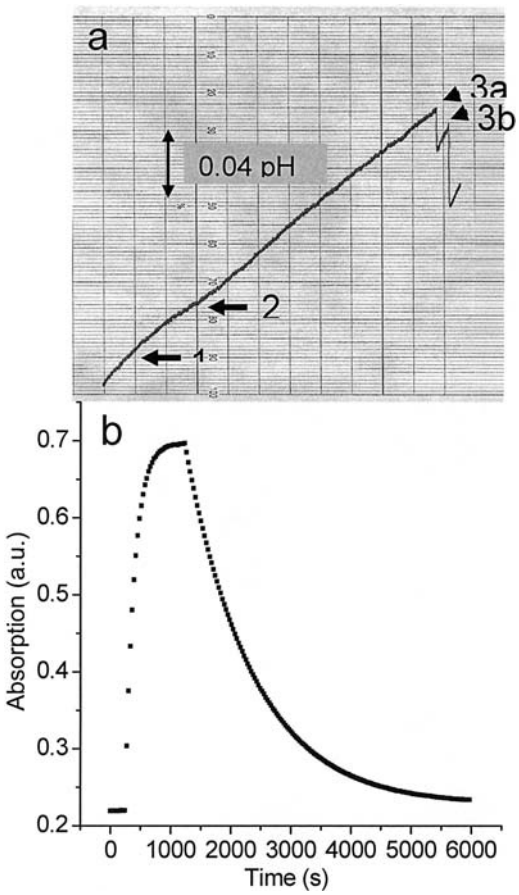

Figure 6. Absence of detectable proton release on formation and decay of the signaling state of AppA, in parallel to UV–Vis absorbance changes. a: Recording of the pH changes during formation and decay of the signaling state of AppA at pH 8.0. Arrows 1 and 2: actinic light on and off, respectively; 3a and 3b: addition of 15 and 30 nmoles of H^+, respectively. The diagonal trend in the trace is due to instrument drift. b: Absorption changes recorded at 495 nm and measured simultaneously. a.u., absorption units.

was confirmed with measurements on the Y17I protein. Parallel absorbance measurements confirmed that the intensity of the blue light was sufficient to drive the majority of the AppA proteins into the signaling state (Fig. 6b).

DISCUSSION

Light sensing in biology is mediated by a limited number of photoreceptor families. Photoreceptor proteins belonging to the rhodopsins, the phytochromes and the xanthopsin family are all activated by light-induced *E/Z* (*i.e*. *trans*/*cis*) isomerization of a particular double bond in their chromophores (*i.e*. retinaldehyde, phytochromobilin and *p*-coumaric acid, respectively [8]). The change in the configuration of such a chromophore leads to changes in the conformation of the surrounding apoprotein, which results in formation of the signaling state. Both the cryptochrome and the phototropin families carry a flavin as chromophore, a compound lacking an isomerizable double bond. For cryptochrome, the mechanism of activation has been postulated to be a light-induced redox reaction involving electron transfer (19) (P. Galland, unpublished), whereas in phototropins light absorption leads to formation of a covalent flavin–cysteinyl adduct (20). With the recent demonstration that AppA functions as a blue-light photoreceptor that antirepresses photosynthesis gene expression in *R. sphaeroides* (6) and the fact that the widely distributed N-terminal flavin binding (BLUF) domain may actually represent a new flavin fold, involved in signal transduction (7), a new family of photoreceptors seems set to emerge.

Our results suggest that the mechanism of signaling state formation in this new family involves the deprotonation of the FAD chromophore, a process in which a conserved tyrosine may function as the proton acceptor. Besides intramolecular proton transfer, there is another interesting parallel between AppA and PYP: both appear to display considerable conformational change between receptor and signaling states (*e.g*. Hoff *et al*. [21]; Masuda and Bauer [6]).

Sequence analysis indicates that the differences observed between the fragment of AppA cloned in the present study and the sequence deposited in the database probably arise from strain differences between *R. sphaeroides* strains HR and RK1. *R. sphaeroides* 2.4.1. strain RK1 is an interesting strain with respect to its motility response to changes in light conditions. Under anaerobic conditions, *R. sphaeroides* responds to a decrease in photosynthetic light intensity by an increase in its stop or reorientation frequency. The photosynthetic apparatus is the photoreceptor for this response (22). In addition, however, the RK1 strain shows a similar increase in its stop frequency on an increase in blue-light intensity, independent of the number of photosynthetic pigments per cell, suggesting that a separate sensor mediates this latter response (23). Interestingly, the genome of *R. sphaeroides* contains, in addition to the gene encoding AppA, two other genes encoding BLUF-domain proteins. One of these (ORF5263) has a chromosomal context in which other putative taxis-related genes are involved. It is therefore tempting to speculate that this latter protein is the photoreceptor for the blue-light motility response displayed by this organism (23).

An intriguing aspect of the manner in which AppA functions is the mechanism of stabilization of its signaling state. In this study, we report that signaling state formation is likely to be based on reversible proton transfer from its flavin cofactor to (an) acceptor(s) in the apoprotein, possibly a tyrosinate. In most biological systems investigated to date, proton transfer reactions have been shown to be rapidly reversible (*e.g*. Hendriks *et al*. [13]). Although we have not yet fully time-resolved the reaction that leads to deprotonation of the flavin, our initial observations indicate that this reaction proceeds faster than the microsecond timescale. As a first-order approximation one would expect the lifetime of the signaling state (or the reprotonation of the flavin) to be of the same order of magnitude. Clearly, the results show that recovery of the signaling state is many orders of magnitude (*i.e*. at least 10^7-fold) slower (see *e.g*. Fig. 2). This paradox shows some similarities with the problem of understanding stabilization of charge separation in photosynthetic reaction centers (*e.g*. Allen, J. P. and. J. C. Williams [24]). Nature has solved this problem by arranging several (electron) acceptors in series. It will be interesting to determine whether a similar solution has evolved in the BLUF family for forward proton transfer. Strikingly, reaction centers appear to use that same solution not only for electrons but also for proton transfer toward their secondary ubiquinone acceptor site (25).

The recovery rate of the receptor state of AppA increases about three-fold on an increase in pH from 8 to 11. This may be caused by a gradual decrease in stability of the receptor state with increasing pH. Titration of AppA from pH 7.5 to 14 revealed that the ground

state was stable over this pH range. Surprisingly, the signaling state of AppA was much more alkaline labile. Flavins in oxidoreductase enzymes often display ''in–out'' conformational transitions. Should this apply to the two states of AppA, the decreased vibrational fine structure (around 415 nm) associated with the signaling state would presumably indicate an ''out'' conformation. Nevertheless, its pK_a is considerably different from the pK_a of FAD in water. This indicates that the flavin must still be in a confined environment. Fluorescence studies may shed further light on this. In view of these properties of the flavin it will also be of interest to determine its redox midpoint potential. Mutation of Tyr-17 into an isoleucine makes the flavin-binding pocket less polarizable. The observed shift in the position and absorbance ratio of the peaks in the flavin absorption spectrum of the mutant protein Y17I is consistent with this.

The spectral difference between the receptor and signaling states is presumably caused primarily by a difference in the protonation state of the flavin. Deprotonation of free flavin results in a 5 nm redshift and an 18 nm blueshift of the absorption maxima of the long- and short-wavelength absorbance band, respectively (22). A 25 nm redshift of the short-wavelength absorbance band is observed between flavin dissolved in Me_2SO and H_2O as a result of increased hydrogen bonding (23). Signaling state formation in AppA involves a redshift in both absorbance bands, suggesting that the postulated deprotonation of FAD is accompanied by an increase in hydrogen bonding, which is in agreement with the loss of vibrational fine structure at the high-energy side of the main UV–Vis transition in the signaling state. The observation that the spectral transition in the longer-wavelength absorption band is slightly different from the corresponding transition of free FAD in aqueous buffer may be explained by the regio-selective protonation of the protein-bound flavin. Nevertheless, additional factors may also contribute, such as the (de)stacking of the flavin with (an) aromatic ring(s) or a cation of nearby amino acid side chains (or both). Such effects will presumably be additive.

The FTIR difference spectrum shows several bands in the 1100–1300 cm^{-1} region. Most of these are affected by the hydrogen bonding to the flavin and have been shown to involve the N3 proton (26). Only part of the bands in the FTIR difference spectrum has been assigned to date. It is possible that both the negative bands at 1443 and 1267 cm^{-1} (atypical for a flavin) and the positive bands at 1453 and 1380 cm^{-1} are due to a tyrosinate to tyrosine transition (see Table 3). Additional bands to be expected in such a transition, but not clearly visible in the FTIR difference spectrum, overlap with flavin peaks or are in the 1500–1700 cm^{-1} region, or both, from which–probably result from excessive IR absorption by water–no identifiable signals were obtained. The absorption peaks in the FTIR spectrum (Fig. 5a) reveal differences in their relaxation characteristics. This may be due to independent contributions by, for example, the flavin and the Amide I absorption of the peptide bonds. Future (time-resolved) FTIR studies with an improved signal to noise ratio will be carried out to reveal whether these differences can be resolved into (an) additionally identifiable state(s) during the recovery of the receptor state of AppA and whether bands can be assigned to a tyrosinate–tyrosine transition.

The studies reported in this communication have been performed with the N-terminal flavin-carrying domain of AppA. This is the part of the protein in which the initial conversion of photon energy into protein conformational changes takes place. To fully understand the photoreceptor function of AppA, it will be very important to extend these studies to full-length AppA. In those studies it will also be possible, and of great interest, to investigate the integration of light and redox signals that regulate expression of the photosynthesis genes of *R. sphaeroides*.

In addition to the Y17L mutation, an Y17F mutation has been constructed. Although the latter is a more conservative replacement, the two mutant proteins are spectroscopically very similar and also Y17F has lost the ability to form a blue-light–induced signaling state.

Table 3. FTIR band positions of tyrosine and tyrosinate. Positions are given in cm^{-1}. Data are from Hienerwadel *et al.* (27)

Tyrosine	Tyrosinate
1616	1600
1600	1560
1518	1499
1451	1443
1376	1413
1290	1355
1248	1330
1179	1273
1111	1174
	1110

Acknowledgements—This work was supported by the Netherlands Organisation for Scientific Research (NWO), through the division of Earth and Life Sciences (Gebied ALW). We thank Dr. S. P. J. Albracht, Dr. J. Brown and Dr. W. Crielaard for helpful reading of the manuscript, Dr. A. Haker for providing the *R. sphaeroides* RK1 genomic DNA and Mr. W. Roseboom for expert help in setting up the FTIR measurements.

REFERENCES

1. Bauer, C., S. Elsen, L. R. Swem, D. L. Swem and S. Masuda (2003) Redox and light regulation of gene expression in photosynthetic prokaryotes. *Philos. Trans. R. Soc. Lond. B. Biol. Sci.* **358**, 147–154.
2. Gregor, J. and G. Klug (1999) Regulation of bacterial photosynthesis genes by oxygen and light. *FEMS Microbiol. Lett.* **179**, 1–9.
3. Oh, J. I. and S. Kaplan (2001) Generalized approach to the regulation and integration of gene expression. *Mol. Microbiol.* **39**, 1116–1123.
4. Braatsch, S., M. Gomelsky, S. Kuphal and G. Klug (2002) A single flavoprotein, AppA, integrates both redox and light signals in *Rhodobacter sphaeroides*. *Mol. Microbiol.* **45**, 827–836.
5. Shimada, H., K. Iba and K. Takamiya (1992) Blue-light irradiation reduces the expression of *puf* and *puc* operons of *Rhodobacter sphaeroides* under semi-aerobic conditions. *Plant Cell Physiol.* **33**, 471–475.
6. Masuda, S. and C. E. Bauer (2002) AppA is a blue light photoreceptor that antirepresses photosynthesis gene expression in *Rhodobacter sphaeroides*. *Cell* **110**, 613–623.
7. Gomelsky, M. and G. Klug (2002) BLUF: a novel FAD-binding domain involved in sensory transduction in microorganisms. *Trends Biochem. Sci.* **27**, 497–500.
8. Hellingwerf, K. J. (2000) Key issues in the photochemistry and signalling-state formation of photosensor proteins. *J. Photochem. Photobiol. B: Biol.* **54**, 94–102.
9. Hellingwerf, K. J. (2002) The molecular basis of sensing and responding to light in microorganisms. *Antonie van Leeuwenhoek* **81**, 51–59.
10. Iseki, M., S. Matsunaga, A. Murakami, K. Ohno, K. Shiga, K. Yoshida, M. Sugai, T. Takahashi, T. Hori and M. Watanabe (2002) A blue-light-activated adenylyl cyclase mediates photoavoidance in *Euglena gracilis*. *Nature* **415**, 1047–1051.
11. Koziol, J. (1971) Fluorometric analysis of riboflavin and its coenzymes. *Methods Enzymol.* **18**, 253–285.
12. Kraayenhof, R., J. J. Schuurmans, L. J. Valkier, J. P. Veen, D. van Marum and C. G. Jasper (1982) A thermoelectrically regulated multipurpose cuvette for simultaneous time-dependent measurements. *Anal. Biochem.* **127**, 93–99.

13. Hendriks, J., I. H. van Stokkum and K. J. Hellingwerf (2003) Deuterium isotope effects in the photocycle transitions of the photoactive yellow protein. *Biophys. J.* **84**, 1180–1191.
14. Kort, R., M. K. Phillips-Jones, D. M. van Aalten, A. Haker, S. M. Hoffer, K. J. Hellingwerf and W. Crielaard (1998) Sequence, chromophore extraction and 3-D model of the photoactive yellow protein from *Rhodobacter sphaeroides*. *Biochim. Biophys. Acta* **1385**, 1–6.
15. Land, E. J. and A. J. Swallow (1969) One-electron reactions in biochemical systems as studied by pulse radiolysis. II. Riboflavin. *Biochemistry* **8**, 2117–2125.
16. Abe, M. and Y. Kyogoku (1987) Vibrational analysis of flavin derivatives: normal coordinate treatment of lumiflavin. *Spectrochimi. Acta A* **43**, 1027–1037.
17. Kim, M. and P. R. Carey (1993) Observation of a carbonyl feature for riboflavin bound to riboflavin-binding protein in the red-excited Raman-spectrum. *J. Am. Chem. Soc.* **115**, 7015–7016.
18. Sasaki, J. and J. L. Spudich (1998) The transducer protein HtrII modulates the lifetimes of sensory rhodopsin II photointermediates. *Biophys. J.* **75**, 2435–2440.
19. Lin, C., D. E. Robertson, M. Ahmad, A. A. Raibekas, M. S. Jorns, P. L. Dutton and A. R. Cashmore (1995) Association of flavin adenine dinucleotide with the *Arabidopsis* blue light receptor CRY1. *Science* **269**, 968–970.
20. Crosson, S. and K. Moffat (2002) Photoexcited structure of a plant photoreceptor domain reveals a light-driven molecular switch. *Plant Cell* **14**, 1067–1075.
21. Hoff, W. D., A. Xie, I. H. Van Stokkum, X. J. Tang, J. Gural, A. R. Kroon and K. J. Hellingwerf (1999) Global conformational changes upon receptor stimulation in photoactive yellow protein. *Biochemistry* **38**, 1009–1017.
22. Grishanin, R. N., D. E. Gauden and J. P. Armitage (1997) Photoresponses in *Rhodobacter sphaeroides*: role of photosynthetic electron transport. *J. Bacteriol.* **179**, 24–30.
23. Kort, R., W. Crielaard, J. L. Spudich and K. J. Hellingwerf (2000) Color-sensitive motility and methanol release responses in *Rhodobacter sphaeroides. J. Bacteriol.* **182**, 3017–3021.
24. Allen, J. P. and J. C. Williams (1998) Photosynthetic reaction centers. *FEBS Lett.* **438**, 5–9.
25. Paddock, M. L., P. Adelroth, G. Feher, M. Y. Okamura and J. T. Beatty (2002) Determination of proton transfer rates by chemical rescue: application to bacterial reaction centers. *Biochemistry* **41**, 14716–14725.
26. Schmidt, J., P. Coudron, A. W. Thompson, K. L. Watters and J. T. McFarland (1983) Hydrogen bonding between flavin and protein: a resonance Raman study. *Biochemistry* **22**, 76–84.
27. Hienerwadel, R., A. Boussac, J. Breton, B. A. Diner and C. Berthomieu (1997) Fourier transform infrared difference spectroscopy of photosystem II tyrosine D using site-directed mutagenesis and specific isotope labeling. *Biochemistry* **36**, 14712–14723.